Limnol. Oceanogr., 56(2), 2011, 599–610

doi:10.4319/lo.2011.56.2.0599

Temperature and nutrient stoichiometry interactively modulate organic matter cycling in a pelagic algal–bacterial community

Julia Wohlers-Zöllner,[a,1,*] Petra Breithaupt,[a] Katja Walther,[b] Klaus Jürgens,[b] and Ulf Riebesell[a]

[a] Leibniz Institute of Marine Sciences (IFM-GEOMAR), Kiel, Germany
[b] Leibniz Institute for Baltic Sea Research, Rostock-Warnemünde, Germany

Abstract

A microcosm experiment was conducted to investigate the interactive effects of rising sea-surface temperature and altered nutrient stoichiometry on the biogeochemical cycling of organic matter in a pelagic algal–bacterial assemblage. Natural seawater, containing a mixed bacterial community, was inoculated with an axenic culture of the bloom-forming diatom species *Skeletonema costatum*. A factorial combination of three temperatures, simulating weak to strong warming as projected for the end of the 21st century, and either nitrogen (N)-replete or -deficient growth conditions were applied. Depending on the type of nutrient limitation, the mixed algal–bacterial communities displayed pronounced differences in the accumulation and microbial utilization of organic matter in response to warming. Under N-deficient conditions, the build-up of organic matter occurred, irrespective of temperature, dominantly in the particulate pool, and only small amounts of dissolved material accumulated. The subsequent bacterial consumption of organic matter was low, as indicated by measurements of bacterial secondary production and extracellular enzyme activities, and remained also largely unaffected by an increase in temperature from 4°C up to 12°C. Contrastingly, warming resulted in a distinct temperature-dependent increase in the accumulation of dissolved organic carbon compounds under N-replete growth conditions. Moreover, rising temperature notably stimulated the bacterial activity, indicating an enhanced flow of organic matter through the microbial loop. These findings suggest that there will be strong shifts in the biogeochemical cycling of organic matter in the upper ocean in response to increased temperature and nutrient loading that will affect pelagic food-web structures and the biological sequestration of organic matter.

Human activities, such as the burning of fossil fuels and changes in land-use practices, are causing major perturbations of the ocean's chemical and physical properties through increased warming and progressive acidification of the upper water layers (Caldeira and Wickett 2003; Barnett et al. 2005; Levitus et al. 2005). These changes in the marine environment are expected to further intensify in the future with, for instance, a projected rise in global surface temperature of 1–6°C by the end of the 21st century (Meehl et al. 2007).

In a recent mesocosm study, surface ocean warming has been shown to directly affect the balance between biological key processes driving the biogeochemical cycling of organic matter in the surface ocean (i.e., autotrophic primary production, heterotrophic consumption and respiration, as well as the sinking of organic matter), due to large discrepancies in their respective temperature sensitivities (Wohlers et al. 2009). Thus, rising sea-surface temperature led to an enhanced heterotrophic consumption of organic carbon (C) relative to autotrophic primary production. Moreover, a pronounced shift in the partitioning of organic C between its particulate and dissolved pools toward the latter was observed. These changes in biogenic C flow ultimately reduced the net community drawdown of CO_2 and lowered the availability of organic C for export, with likely consequences for pelagic food-web structure and the efficiency of biogenic C sequestration to depth via the biological pump.

In addition to this, surface ocean warming and other anthropogenic climate change stressors are expected to affect the marine biota by disturbing the major nutrient cycles (e.g., nitrogen [N] and phosphorus [P]). For instance, the projected intensifying of water-column stratification (Sarmiento et al. 1998) and progressing ocean acidification (Feely et al. 2009) have been shown in modeling and experimental laboratory studies to enhance the biological fixation of molecular nitrogen (N_2) by diazotrophic cyanobacteria (Boyd and Doney 2002; Barcelos e Ramos et al. 2007; Hutchins et al. 2007), thereby increasing the availability of N relative to P. Further complicating the picture, human activities have led to increased inputs of allochthonous nutrients via river-runoff and atmospheric dust deposition along the coasts (Jickells 1998; Falkowski et al. 2000) as well as to changes in the relative abundance of these nutrients through coastal water management practices, currently resulting in rising N : P ratios (Jickells 1998). This man-made effect is also expected to strengthen in coming decades due to changes in global precipitation patterns (Trenberth et al. 2007). Although primary productivity is generally considered to be limited by N throughout most of the ocean (Falkowski 1997; Tyrrell 1999), a seasonal P-limitation has been suggested in various regions (e.g., strongly freshwater-influenced coastal zones or enclosed oceanic areas such as the Baltic Sea [Zweifel et al. 1993], the subtropical gyres in the North Pacific [Karl et al. 2001], and the Atlantic Ocean [Ammerman et al. 2003], as well as the eastern Mediterranean Sea [Thingstad et al.

* Corresponding author: julia.wohlers@bio.uib.no

[1] Present address: Department of Biology, University of Bergen, Bergen, Norway

2005]). The expected rise in N- compared to P-loading due to anthropogenic climate change may, thus, further enhance the potential for P-limitation in such areas.

The type of prevailing nutrient limitation (i.e., N- vs. P-limited growth), can have pronounced effects on the magnitude, composition, and microbial utilization of organic matter during algal blooms, as has been shown by several laboratory studies (Obernosterer and Herndl 1995; Puddu et al. 2003; Magaletti et al. 2004). For instance, P-limited growth conditions led to a distinctly higher algal release of dissolved organic carbon (DOC), in particular of carbohydrates, compared to N-limited and nutrient-replete conditions (Obernosterer and Herndl 1995; Magaletti et al. 2004). Moreover, severe P-deficiency (N : P = 100–145; Obernosterer and Herndl 1995; Puddu et al. 2003) also markedly reduced the efficiency of the associated bacterial communities to utilize the released material.

Thus, both sea-surface warming and the availability of inorganic nutrients have been shown separately to exert a marked effect on the autotrophic build-up and subsequent heterotrophic consumption of organic matter in the surface ocean. To investigate their interactive synergistic or antagonistic effects on marine pelagic microbial communities and the associated biogeochemical cycling of organic matter, a microcosm study was conducted, using an assemblage of the bloom-forming diatom species *Skeletonema costatum* and a mixed Baltic Sea bacterial community. Here, we present results on the build-up, composition, and degradability of organic matter.

Methods

Experimental design and sampling procedure—The microcosm experiment was conducted from 05 July to 13 August 2007 at the Leibniz Institute of Marine Sciences in Kiel, Germany. The microcosms consisted of acid-cleaned and autoclaved 25-liter polycarbonate bottles (Nalgene).

Natural seawater was collected in late spring at the Booknis Eck station in Kiel Bight at a depth of ~ 10 m (original water temperature ~ 6–7°C), and allowed to age in the dark for several weeks. Before use in the experiment, the water was prefiltered through precombusted (450°C, 5 h) GF/F- (glass fiber filter; Whatman) and 0.45-μm cellulose acetate filters in order to retain a mixed natural bacterial community. Eighteen bottles in total were each filled with 24 liters of the filtered water and equally distributed onto three temperature-controlled climate chambers. The temperature (T) of the chambers was adjusted to 4°C, 8°C, and 12°C, respectively, simulating weak to strong warming as projected for the winter season in the Baltic Sea region until the end of the 21st century (4–10°C; Giorgi et al. 2001). The communities were preadapted to the respective temperatures for several days prior to the experiment.

Regular determination of bacterial and heterotrophic nanoflagellate (HNF) abundance during the filtration process confirmed the absence of flagellate grazers and a negligible reduction in bacterial cell numbers with an initial bacterial abundance of $0.49 \times 10^6 \pm 0.04 \times 10^6$ cells mL^{-1}. A major influence of HNF on algal–bacterial community dynamics is regarded to be unlikely as based on observed low abundances during the relevant periods of the experiment (i.e., < 750 individuals mL^{-1}; except for the warmest temperature treatment of the N-replete microcosms, where HNF abundance increased to ~ 3400 individuals mL^{-1} on the last day included in the calculations).

Before the start of the experiment, the bottles were inoculated with an axenic culture of the diatom species *Skeletonema costatum* (CCMP 1332), yielding an initial algal density of ~ 1000 cells mL^{-1}. *Skeletonema costatum* is one of the dominant algal species forming the yearly phytoplankton spring bloom in Kiel Bight, and has been the most abundant species in a previous mesocosm experiment (Wohlers et al. 2009). Microscopic analysis using the Utermöhl method (Utermöhl 1958) at selected time points confirmed that *Skeletonema* was the dominant algal species growing in the microcosms (in some mesocosms few *Nitzschia*-like cells were observed in neglectable densities of < 600 cells mL^{-1} compared to maximum cell abundances of up to 70,000 cells mL^{-1} for *Skeletonema*). Initial dissolved inorganic nutrient concentrations were 5.4 μmol L^{-1} nitrate (NO_3^-), 0.4 μmol L^{-1} nitrite (NO_2^-), 1.7 μmol L^{-1} ammonium (NH_4^+), 0.3 μmol L^{-1} phosphate (PO_4^{3-}), and 5.9 μmol L^{-1} silicate [$Si(OH)_4$].

In order to establish two different nutrient regimes, one half of the bottles received only additional PO_4^{3-}, whereas the other half received both PO_4^{3-} and NO_3^-, yielding final concentrations of 0.87 ± 0.06 μmol L^{-1} dissolved inorganic phosphorus (DIP) and of 7.5 ± 0.7 μmol L^{-1} and 25.9 ± 0.6 μmol L^{-1} dissolved inorganic nitrogen (DIN), respectively. This resulted in initial N : P ratios of ~ 9 : 1 ('N-deficient' treatment) and 30 : 1 ('N-replete' treatment). Dissolved silicic acid [$(SiOH)_4$] was added at a final concentration of 44 μmol L^{-1}, thereby ensuring silica-replete conditions. The seawater was further amended with trace metals, vitamins, and selenium in f/10 amounts (Guillard and Ryther 1962).

All treatments were run in triplicates. The bottles were placed horizontally below light benches. These contained full-spectrum light tubes covering the complete range of photosynthetically active radiation. The light benches were controlled by separate computer units, generating a triangular light curve (i.e., light intensities increased until midday and decreased thereafter) with an overall light : dark cycle of 12 : 12 h. Using a 4π-light sensor (LiCor), maximum light intensities of 377 ± 19 μmol photons m^{-2} s^{-1} were measured at midday. In order to provide identical light conditions, the position of the bottles rotated every day. Prior to sampling, each bottle was gently agitated with a magnetic stirrer for ~ 1 min.

Biogeochemical analyses—Chlorophyll *a* (Chl *a*) was determined fluorometrically on a Turner 10-AU fluorometer (Welschmeyer 1994). For this purpose, 50–100 mL of sample were filtered onto combusted (450°C, 5 h) GF/F-filters (Whatman) and stored in polypropylene tubes at −20°C. Prior to analysis, Chl *a* was extracted in 90% acetone.

The concentrations of the dissolved inorganic nutrients NO_3^-, NO_2^-, PO_4^{3-}, and $Si(OH)_4$ were analyzed colori-

metrically from filtered (cellulose acetate filters, 5-μm pore size) water samples following the protocol of Hansen and Koroleff (1999). Ammonium was determined from unfiltered water samples (Holmes et al. 1999). All nutrient analyses were carried out on the day of sampling except for the last two sampling occasions, where samples were filtered and stored at -20°C until analysis.

For the determination of particulate organic carbon (POC), particulate organic nitrogen (PON), and particulate organic phosphorus (POP) 100–200 mL of sample were filtered onto precombusted (450°C, 5 h) GF/F-filters (Whatman) and stored at -20°C until analysis. Prior to analysis on a Eurovector EuroEA-3000 elemental analyzer (Sharp 1974), POC and PON samples were dried at 60°C for 6 h. POP concentrations were determined colorimetrically after oxidation with peroxodisulphate (Hansen and Koroleff 1999).

DOC and dissolved carbohydrates were analyzed from the GF/F-filtrate of the particulate samples. The filtrate was collected in precombusted (450°C, 12 h) 20-mL glass ampoules and frozen at -20°C. The analysis of DOC was carried out on a Shimadzu Total Organic Carbon analyzer (TOC_{VCN}) using the High Temperature Combustion Oxidation method (Qian and Mopper 1996). The concentration of dissolved polysaccharides (PCHO) was measured spectrophotometrically using the 2,-4,-6-tripyridyl-s-triazine approach (Myklestad et al. 1997).

Microbial parameters—Bacterial Secondary Production (BSP) was assessed through the incorporation of ^{3}H-leucine following the protocol of Simon and Azam (1989). Ten milliliters of sample were spiked with 50 μL of radioactively labeled ^{3}H-leucine (specific activity 77 μCi nmol^{-1}) and 50 μL of unlabeled leucine, yielding a final concentration of 106 nmol leucine L^{-1}. Duplicate samples plus an additional formalin-killed control were dark-incubated at in situ temperature (i.e., in the respective climate chamber) for 1.5–3 h. The incubation was terminated by adding formaldehyde (1% v : v final concentration). Samples were filtered onto 0.2-μm polycarbonate filters, rinsed with ice-cold trichloroacetic acid solution (5%) and subsequently radioassayed in 4 mL of scintillation cocktail (Lumagel plus) on a Packard TriCarb scintillation counter. ^{3}H-leucine incorporation (pmol L^{-1} h^{-1}) was converted into BSP (μg C L^{-1} h^{-1}) by applying a theoretical conversion factor of 3.1 kg C mol^{-1} leucine (Simon and Azam 1989).

The maximum hydrolytic activities (V_{max}) of the bacterial extracellular enzymes β-D-glucosidase (β-D-gluc), leucine-aminopeptidase (leu-amp), butoxycarbonyl-phenylalanine-serine-arginine-peptidase (BOC-pep), as well as alkaline phosphatase (APA) were determined following the protocol of Hoppe (1983). Subsamples of 200 μL each were pipetted in quadruplicate into microtiter plates. Fluorogenic model substrates (i.e., 4-methylumbelliferyl-β-D-glucopyranoside [MUF-β-D-glucoside; Sigma-Aldrich], L-leucine-4-methyl-7-coumarinylamide [leu-MCA; Sigma-Aldrich], butoxycarbonyl-phenylalanine-serine-arginine-4-methyl-7-coumarinylamide [BOC-MCA; Pepta Nova GmbH], and 4-methylumbelliferryl-phosphate [MUF-phosphate, Sigma-Aldrich]) were added to the samples at a saturating concentration of 250 μmol L^{-1}. Sample fluorescence was determined immediately after addition of the substrates by using a microtiter plate fluorometer (Fluoroskan Ascent, Ascent Software; excitation 364 nm, emission 445 nm), as well as after a dark-incubation period of $\sim$ 3 h at in situ temperature. Fluorescence signals were converted into maximum hydrolytic enzyme activities (V_{max}; in μmol L^{-1} h^{-1}) by using empirical conversion factors, which were determined from fluorescence readings of defined concentrations of MUF and MCA (P. Breithaupt pers. comm.).

Calculations

Cardinal points of the bloom: For a better comparison of the various temperature and nutrient treatments, three characteristic bloom phases (i.e., 'prebloom,' 'bloom peak,' and 'postbloom') were identified on the basis of changes in Chl *a* concentration [Chl *a*]. To determine the day of bloom onset and, thus, the transition from prebloom to bloom peak, the natural logarithm (ln) of Chl *a* was calculated and plotted against time. During the exponential growth of algal cells, ln [Chl *a*] should scale linearly with time. Thus, the first data point fulfilling this linearity criterion was defined as the day of bloom onset. The end of the bloom phase was defined as the day of maximum Chl *a* in the respective microcosms. The bloom peak was accelerated by 1.75 d $^{\circ}$C^{-1} in both N-replete and N-deficient treatments. The postbloom phase started with the first day after the respective Chl *a* peak. Because the development was slowed down at low temperature, the sampling period did not fully cover the degradation phase in the 4°C treatments, hence yielding higher biomass concentrations on the last day of sampling at 4°C compared to elevated temperatures. To exclude possible temperature-artefacts when calculating, for instance, time-integrated means of bacterial activity for the postbloom phase, the last day included in the calculations was day 42 (i.e., the last day of sampling), day 35 in the 8°C, and day 27 (N-replete)/24 (N-deficient) in the 12°C treatments.

Algal growth rate based on Chl *a* ($\mu_{Chl\ a}$) : $\mu_{Chl\ a}$ was calculated for the period of exponential growth based on changes in Chl *a* concentration according to: $\mu_{Chl\ a} = (\ln [Chl\ a_{t2}] - \ln [Chl\ a_{t1}]) / (t_2 - t_1)$, with t_1 being the first day of exponential growth and t_2 being the last day of exponential growth.

POM build-up: The maximum net build-up of POC (ΔPOC), PON (ΔPON), and POP (ΔPOP) in units of μmol C, N, and P L^{-1}, respectively, was determined by calculating the difference between the initial (day 0) and the maximum concentration. The initial concentration was averaged over all microcosms.

DOM build-up: The rate of increase in polysaccharide concentration [V_{incr} (PCHO)] was determined by applying a linear regression model to the individual data sets for the time period from DIP or DIN exhaustion to the end of the experiment.

To account for the differences in biomass formation between the P- and N-lim treatments, the net build-up of PCHO (ΔPCHO) was normalized to the maximum net

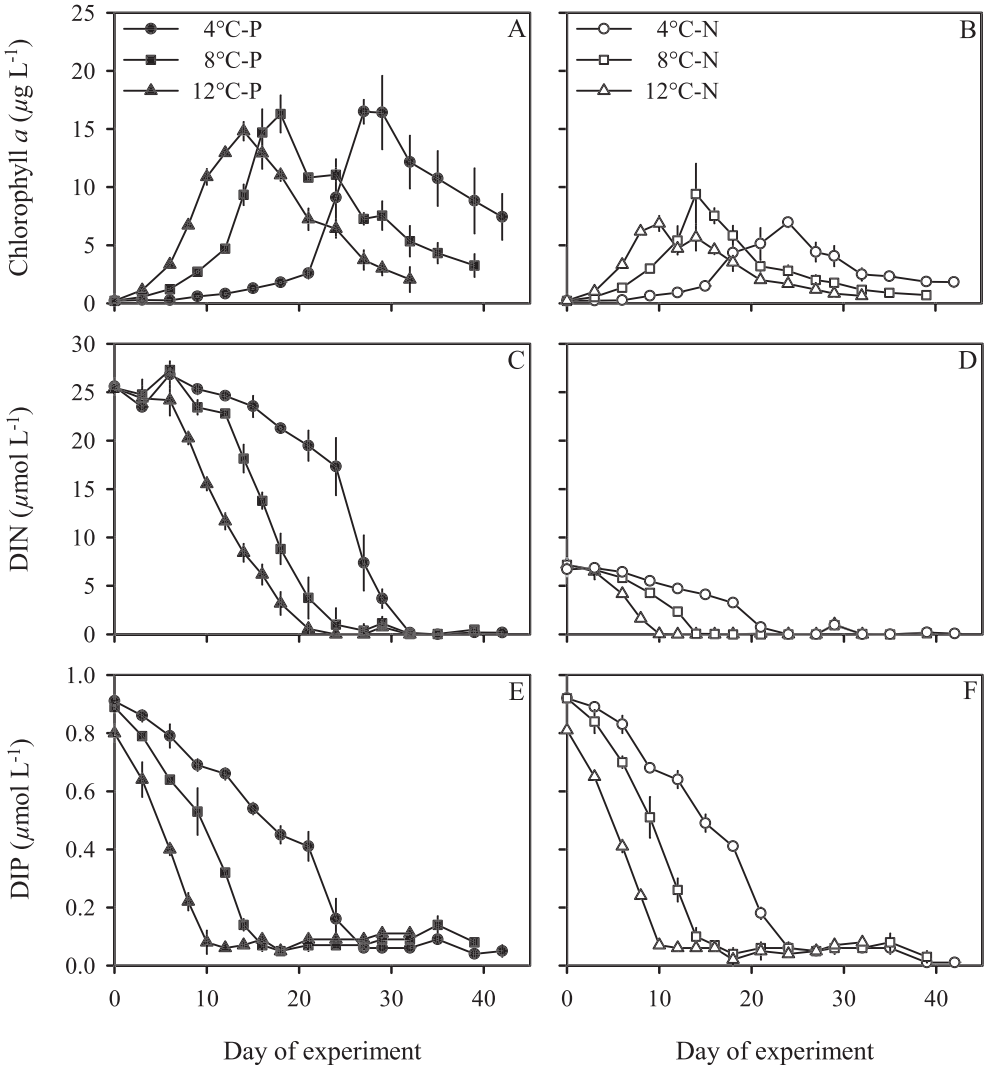

Fig. 1. Temporal development of (A, B) chlorophyll *a* (Chl *a*), (C, D) dissolved inorganic nitrogen (DIN), and (E, F) dissolved inorganic phosphorus (DIP) in the N-replete (closed symbols) and N-deficient treatments (open symbols). Lines represent the average of three replicate microcosms ± SD.

accumulation of POC (ΔPOC). ΔPCHO was calculated according to: $\Delta PCHO = (PCHO_e - PCHO_i)$, with i referring to the initial PCHO concentration (averaged from day 0 until the onset of nutrient exhaustion), and e referring to the PCHO concentration at the end of the bloom (i.e., days 42, 35, and 27 [N-replete] / 24 [N-deficient] at 4°C, 8°C, and 12°C).

Statistical analysis—Treatment effects between P- and N-deficient microcosms were tested using one-way ANOVA (Statistica). Temperature effects were assessed by linear regression analysis (Model I type; SigmaPlot), with the slope m describing the direction and magnitude of change in various parameters (e.g., algal growth rate, timing of the bloom peak, net build-up of particulate organic matter, V_{max} of bacterial extracellular enzymes) with increasing temperature. A statistical significance level of $p < 0.05$ was applied to all tests.

Results

Initial nutrient availability and algal bloom development—After the addition of inorganic nutrients, thereby creating two differing N : P regimes of 30 : 1 (N-replete) and 9 : 1 (N-deficient), the development of phytoplankton blooms was observed in all treatments. The onset of algal growth was marked by a rapid decline of inorganic nutrients and a simultaneous increase in Chl *a* concentration (Fig. 1). Rising temperature affected the temporal development of the bloom with a doubling of Chl *a*–specific algal growth rates from 0.2 d^{-1} at 4°C to 0.4 d^{-1} at 12°C, an accelerated uptake of inorganic nutrients, and a forward shift of the bloom peak by ~ 1.75 d $°C^{-1}$ (Fig. 1; Table 1). Maximum Chl *a* concentrations of 16.2 ± 1.9 µg Chl *a* L^{-1} and 7.8 ± 1.8 µg Chl *a* L^{-1} were achieved in the N-replete and N-deficient treatments, respectively, thus yielding about twice the biomass under the former conditions (Fig. 1A,B). In

Table 1. Autotrophic growth and temporal development of the bloom. Algal growth rates ($\mu_{Chl\ a}$; units of μg Chl *a* d^{-1}) were determined during exponential growth based on chlorophyll *a* (Chl *a*) measurements. The bloom peak describes the day of maximum Chl *a* concentration. Values represent the average of three replicate microcosms ± SD. The effect of temperature on algal growth rates and the timing of the bloom peak were assessed using linear regression analysis.

	4°C	8°C	12°C	m	R^2	*p*
$\mu_{Chl\ a}$						
High-N	0.20±0.0	0.27±0.01	0.43±0.0	0.02	0.96	<0.0001*
Low-N	0.18±0.0	0.27±0.02	0.42±0.01	0.02	0.83	0.001*
Bloom peak						
High-N	28±1	18±0	14±0	−1.71	0.94	<0.0001*
Low-N	24±0	14±0	9±1	−1.83	0.95	<0.0001*

* Indicates significant temperature effects.

contrast, a notable effect of temperature on maximum Chl *a* was not observed. Independent of the type of nutrient limitation, DIN and DIP were both depleted until the detection limit in all microcosms (Fig. 1C–F). Elevated maximum hydrolytic activities of the organic P-cleaving enzyme alkaline phosphatase [V_{max} (APA)] in the high-N compared to the low-N treatments, however, indicate a pronounced P deficiency under the former conditions. Moreover, experimental warming seemed to further enhance the degree of P limitation in the N-replete microcosms, because the average V_{max} (APA) significantly increased with rising temperature ($p = 0.002$), whereas it did not display a significant temperature response under N-deficient conditions.

Build-up of particulate and dissolved organic matter pools—The increase in Chl *a* was closely followed by the build-up of particulate organic matter (Fig. 2). POC concentrations increased from initially 4.1 ± 0.5 μmol C L^{-1} to maximum values of 438.9 ± 51.6 μmol C L^{-1} and 283.2 ± 53.9 μmol C L^{-1} under N-replete and -deficient conditions, respectively (Fig. 2A,B). Overall, the build-up of POC exceeded the C production estimated from initial nutrient concentrations and assuming Redfield stoichiometry of C : N : P = 106 : 16 : 1 (Redfield et al. 1963) substantially by a factor of ~ 4.8 and ~ 5.7 in the high-N and low-N microcosms, respectively.

While POC concentrations reached a plateau and remained high until the end of the experiment in the N-replete treatments at 4°C and 8°C, a pronounced decrease in POC was observed at the highest temperature of 12°C from day 24 onward (Fig. 2A), yielding a net loss of ~ 160 μmol C L^{-1}. In contrast, a similar degradation signal was not observed in the respective N-deficient treatment (Fig. 2B).

The temporal development of PON (Fig. 2C,D) and POP concentrations (Fig. 2E,F) closely followed the drawdown of the corresponding dissolved inorganic nutrients. The maximum net build-up of PON (ΔPON) ranged between 22.6 μmol N L^{-1} (12°C) and 24.7 μmol N L^{-1} (4°C) in the high-N treatments and between 8.4 μmol N L^{-1} (12°C) and 10.8 μmol N L^{-1} (4°C) in the low-N treatments, hence showing a slight, but not statistically significant, decrease with rising temperature (Table 2). Under the latter conditions, ΔPON also exceeded the initially available amount of DIN of 7.5 ± 0.7 μmol N L^{-1}, indicating the utilization of an additional N source. In line with this, the pool of dissolved organic nitrogen (DON) showed a continuous decline in the course of the experiment of, on average, 4.8 ± 0.7 μmol L^{-1} (data not shown).

For POP, a net build-up (ΔPOP) of 0.61–0.71 μmol P L^{-1} was observed, with significantly lower values under N-replete compared to N-deficient conditions (one-way ANOVA: $p = 0.01$). Moreover, rising temperature led to a significant decrease of ΔPOP in the high-N treatments (Table 2; $p = 0.04$), whereas it had no effect under low-N conditions (Table 2; $p = 0.54$). After the phase of exponential algal growth, PON and POP concentrations remained high until the end of the experiment in all treatments, although with a certain variability.

In the N-replete microcosms, a concurrent increase in both bulk DOC and PCHO concentration occurred shortly after the onset of phosphate depletion (Fig. 3A,C). Here, rising temperature significantly enhanced the accumulation of dissolved C compounds, as illustrated by the slope of PCHO increase [V_{incr} (PCHO); Table 3, $p = 0.02$]. In contrast, DOC and PCHO concentrations increased only weakly in the N-deficient treatments and were not notably affected by warming (Fig. 3B,D; Table 3). To account for the differences in biomass development between the nutrient treatments, the net accumulation of PCHO was normalized to the respective maximum biomass accumulating in the water column (i.e., ΔPOC). This analysis revealed that ΔPCHO accounted, independent of ambient temperature, for 2.3–5.6% of ΔPOC under N-deficient conditions, whereas this proportion significantly increased in response to warming from 4.1% at 4°C up to 14.1% at 12°C under N-replete conditions ($p = 0.03$; Table 3).

Microbial activities—In close temporal connection to the development of algal biomass, an increase in bacterial secondary production (BSP) was observed (Fig. 4), yielding already within the first few days of the experiment a clear temperature signal of higher BSP rates at elevated temperatures. Although BSP rates further increased after this first impulse in the high-N treatments (Fig. 4A), they rapidly leveled off in the N-deficient treatments and remained stable at low activities until the end of the

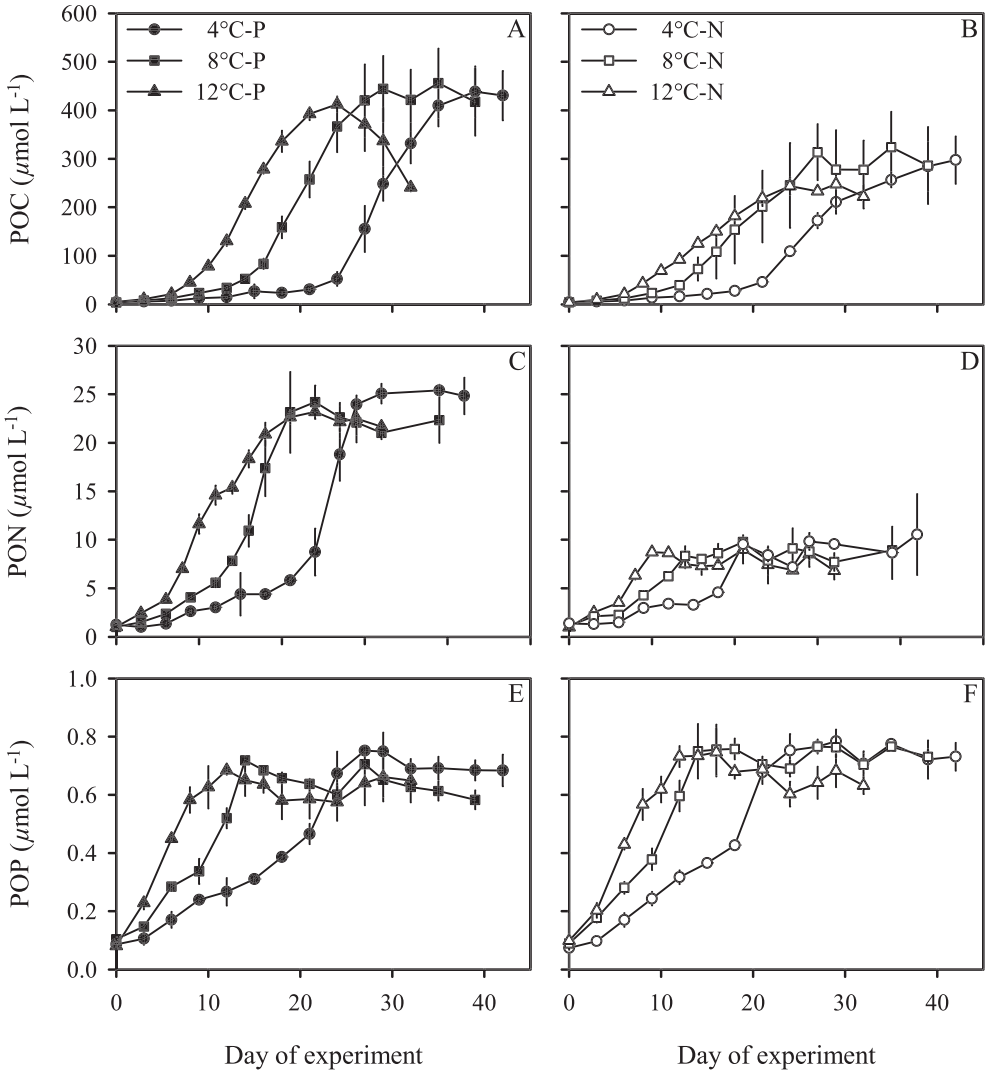

Fig. 2. Build-up of (A, B) particulate organic carbon (POC), (C, D) nitrogen (PON), and (E, F) phosphorus (POP) in the N-replete (closed symbols) and N-deficient (open symbols). Lines represent the average of three replicate microcosms ± SD.

Table 2. Maximum net build-up of particulate organic carbon (ΔPOC), nitrogen (ΔPON), and phosphorus (ΔPOP) (in μmol L^{-1}). Values represent the average of three replicate microcosms ± SD. The effect of temperature on ΔPOC, ΔPON, and ΔPOP was assessed using linear regression analysis.

	4°C	8°C	12°C	m	R^2	p
ΔPOC						
High-N	435.3±53.0	459.8±75.2	409.2±16.7	−3.30	0.05	0.57
Low-N	294.6±46.4	297.1±83.0	245.7±7.6	−6.10	0.16	0.30
ΔPON						
High-N	24.7±0.4	23.5±2.4	22.6±0.6	−0.27	0.35	0.09
Low-N	10.8±3.0	9.1±0.9	8.4±1.3	−0.30	0.26	0.16
ΔPOP						
High-N	0.68±0.06	0.61±0.01	0.61±0.02	−0.01	0.47	0.04*
Low-N	0.71±0.03	0.71±0.07	0.68±0.05	0.00	0.06	0.54

* Indicates significant temperature effects.

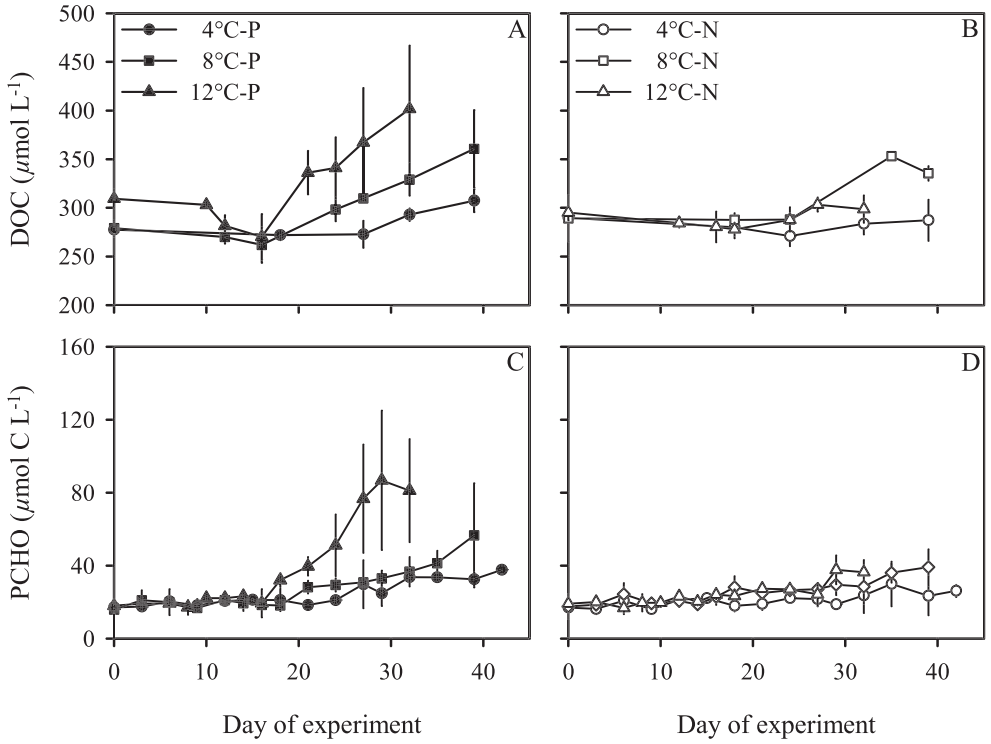

Fig. 3. Build-up of (A, B) dissolved organic carbon (DOC) and (C, D) dissolved polysaccharides (PCHO) in the N-replete (closed symbols) and N-deficient (open symbols). Lines represent the average of three replicate microcosms ± SD.

experiment (Fig. 4B). For a better comparison of bacterial degradative activities, time-integrated mean values of BSP and maximum hydrolytic activities of the bacterial extracellular enzymes β-D-gluc, leu-amp, and BOC-pep were calculated for each replicate during the postbloom phase (Fig. 5; Table 4; *see* also Methods for details on calculations). While average BSP rates showed a significant positive response to warming under both N-replete and -deficient conditions (Fig. 5A), markedly higher values and a generally stronger relation to temperature were observed in the high-N microcosms. Thus, BSP rates increased by a factor of ~ 2.5 from 4.5 ± 0.2 μg C L^{-1} h^{-1} at 4°C to 11.2 ± 1.9 μg C L^{-1} h^{-1} at 12°C under N-replete conditions, whereas they hardly doubled with a temperature rise of 8°C from 2.3 ± 0.7 μg C L^{-1} h^{-1} to 4.4 ± 0.4 μg C L^{-1} h^{-1} in the N-deficient treatments (Fig. 5A; P-lim: $p = 0.009$; N-lim: $p = 0.008$).

Table 3. Dissolved polysaccharides (PCHO). Given are the rate of PCHO accumulation [V_{incr} (PCHO); in μmol C L^{-1} d^{-1}] as well as the ratio between maximum net PCHO build-up and maximum net accumulating biomass (ΔPCHO : ΔPOC; in %). Values represent the average of three replicate microcosms ± SD. The effect of temperature on these variables and parameters was assessed using linear regression analysis.

	4°C	8°C	12°C	m	R^2	p
V_{incr} (PCHO)						
High-N	0.8±0.3	1.4±0.7	3.2±1.6	0.30	0.57	0.02*
Low-N	0.4±0.1	0.6±0.4	0.7±0.2	0.03	0.16	0.29
ΔPCHO : ΔPOC						
High-N	4.1±1.2	5.2±0.2	14.1±7.3	1.3	0.52	0.03*
Low-N	2.3±1.4	5.6±0.9	3.2±1.1	0.12	0.05	0.56

* Indicates significant temperature effects.

Similarly, also the mean maximum hydrolytic rates of β-D-gluc (Fig. 5B) and leu-amp (Table 4) displayed significantly higher values (one-way ANOVA: β-gluc: $p < 0.0001$, leu-amp: $p = 0.002$) as well as a distinct, although not uniform, response to warming under high-N conditions. Thus, V_{max} rates of β-D-gluc increased significantly with rising temperature from 0.032 ± 0.002 μmol L^{-1} h^{-1} at 4°C to 0.056 ± 0.001 μmol L^{-1} h^{-1} at 12°C ($p = 0.02$), whereas the V_{max} rates of leu-amp showed a significant decline by a factor of ~ 2 from 1.55 ± 0.20 μmol L^{-1} h^{-1} at 4°C to 0.81 ± 0.01 μmol L^{-1} h^{-1} at 12°C ($p < 0.001$). Analogous to this negative correlation with temperature also, the ratio of leu-amp to BOC-pep showed a significant decrease with rising temperature from 26.68 ± 5.94 at 4°C to 3.90 ± 0.93 at 12°C (Table 4; $p < 0.001$). In contrast to the N-replete microcosms, the maximum hydrolytic activity of β-D-gluc and leu-amp remained unaffected by rising temperature under low-N conditions with average values of 0.021 ± 0.006 μmol L^{-1} h^{-1} and 0.75 ± 0.16 μmol L^{-1} h^{-1}, respectively (Fig. 5B; Table 4).

Discussion

Algal bloom development—Through addition of inorganic nutrients, two differing N : P regimes were successfully established, resulting in either N-replete or N-deficient growth conditions. In the course of the experiment, distinct

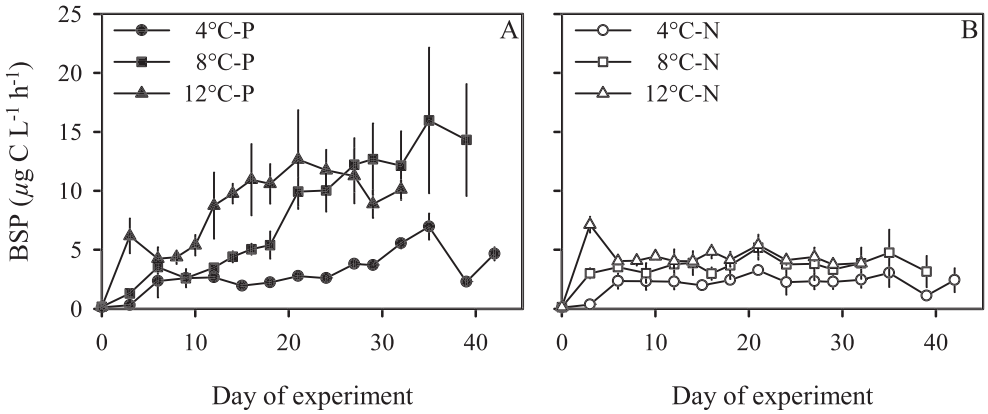

Fig. 4. Temporal development of bacterial secondary production (BSP) in the (A) N-replete (closed symbols) and (B) N-deficient treatments (open symbols). Lines represent the average of three replicate microcosms ± SD.

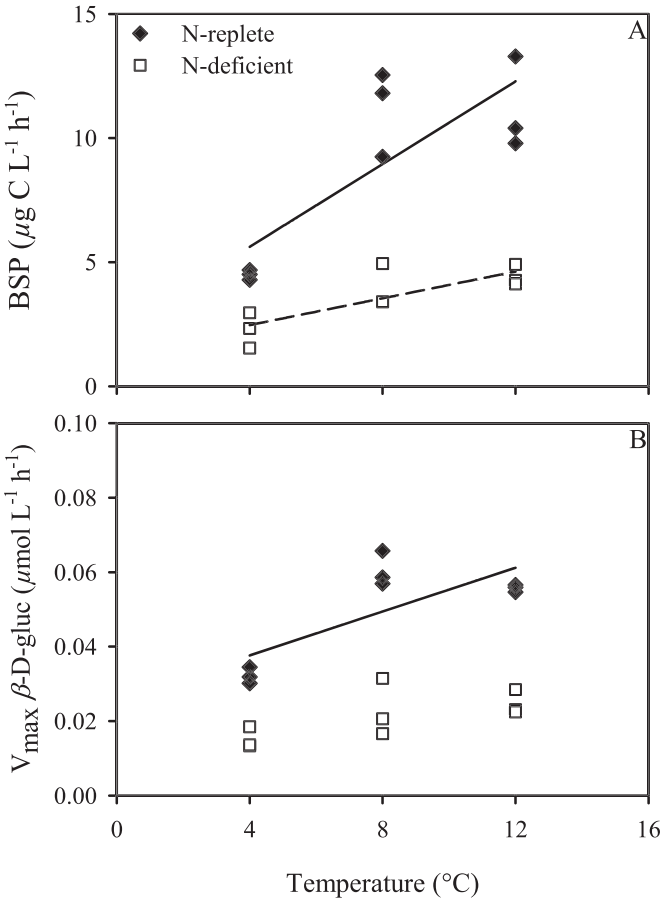

Fig. 5. Temperature-dependency of (A) BSP and (B) maximum hydrolytic activity of the bacterial hydrolytic enzyme β-D-glucosidase (V_{max} β-D-gluc) during the postbloom phase. N-replete treatments are displayed as closed diamonds, the N-deficient treatments as open squares. Solid lines represent significant ($p < 0.05$) linear regressions ($n = 9$; N-replete: BSP = 0.83T + 2.28, $R^2 = 0.65$, $p = 0.009$; β-D-gluc = 0.003T − 0.026, $R^2 = 0.58$, $p = 0.017$; N-deficient: BSP = 0.27T + 1.39, $R^2 = 0.66$, $p = 0.008$; β-D-gluc: not significant).

blooms of *Skeletonema costatum* developed in all treatments. Increasing the temperature by 4–8°C led to an acceleration of bloom timing as evidenced by elevated Chl *a*–based algal growth rates, an accelerated nutrient uptake, and an earlier bloom peak. The magnitude of algal biomass accumulation, as depicted by maximum Chl *a* concentration, was independent of ambient temperature, but displayed approximately two-fold higher values in N-replete compared to N-deficient treatments. Similarly, also primary production rates did not reveal a significant temperature effect (Breithaupt 2009). The lack of a pronounced response of autotrophic biomass accumulation and bloom timing to experimental warming is consistent with findings from previous indoor-mesocosm studies using natural plankton communities, where an increase in temperature of 2–6°C also led to a temporal advancement of the spring bloom by 1.0–1.4 d $°C^{-1}$ (Sommer and Lengfellner 2008; Wohlers et al. 2009). Because the timing of the spring bloom in natural environments can vary considerably by several weeks between years, the observed acceleration of autotrophic growth is likely negligible from an ecological point of view. Similarly, a noticeable effect of ocean warming on the temporal onset of the diatom spring bloom was not detected in a long-term data set from the North Sea (Edwards and Richardson 2004).

Build-up and elemental composition of particulate organic matter—Concomitant to the rapid decline in dissolved inorganic nutrients and the rise in Chl *a* concentration, a pronounced increase in the pools of POC, PON, and POP occurred in all treatments. Although experimental warming had no effect on the maximum build-up of POC and PON, the net accumulation of POP displayed a pronounced response to both altered nutrient availability and increasing temperature. Thus, ΔPOP was not only markedly lower under N-replete compared to N-deficient conditions, accounting for 73.1% ± 5.5% and 80.4% ± 5.6% of available DIP, respectively, but was also significantly reduced by rising temperature in the former treatments.

Table 4. Maximum hydrolytic activity (V_{max}; in μmol L^{-1} h^{-1}) of bacterial extracellular enzymes. Given are the average maximum hydrolytic activities of alkaline phosphatase (APA) over the entire bloom period and of leucine aminopeptidase (leu-amp), BOC-peptidase (BOC-pep), and the ratio of leu-amp to BOC-pep (leu-amp : BOC-pep) during the postbloom phase. The activity of BOC-pep was only investigated in the high-N treatments. Values represent the average of three replicate microcosms ± SD. The effect of temperature on these variables and parameters was assessed using linear regression analysis. na = not analyzed.

	4°C	8°C	12°C	m	R^2	p
V_{max} (APA)						
High-N	0.14±0.01	0.15±0.02	0.21±0.02	0.01	0.76	0.002*
Low-N	0.12±0.0	0.13±0.03	0.14±0.01	0.00	0.30	0.13
V_{max} (leu-amp)						
High-N	1.55±0.20	1.38±0.09	0.81±0.01	−0.09	0.83	0.001*
Low-N	0.89±0.18	0.69±0.13	0.67±0.08	−0.03	0.36	0.09
V_{max} (BOC-pep)						
High-N	0.12±0.01	0.18±0.08	0.22±0.05	0.01	0.44	0.0497*
Low-N	na	na	na	na	na	na
Leu-amp : BOC-pep						
High-N	26.68±5.94	13.86±4.89	3.90±0.93	−2.85	0.86	<0.001*
Low-N	na	na	na	na	na	na

* Indicates significant temperature effects.

While POP and PON concentrations remained, thereafter, high until the end of the experiment, a pronounced decrease was observed for POC at the most elevated temperature of the high-N microcosms, which was, however, not mirrored in the respective low-N microcosms. Most likely, these observations result from shifts in the heterotrophic degradation of organic compounds. In line with this, the N-replete treatments displayed distinctly higher rates of BSP, the organic-P–cleaving algal and bacterial enzyme APA, and other C-specific extracellular enzymes. Moreover, these activities were clearly stimulated by warming under high-N conditions, whereas this temperature effect was substantially dampened or even nonexistent in the respective N-deficient treatments. The indicated rapid remineralization and efficient reutilization of P, thereby refueling the organic P pool, may, however, partly represent a side effect of the experimental set-up, which did not allow for sedimentation of detrital material out of the water column.

C partitioning between dissolved and particulate organic matter—In the N-replete treatments, a marked increase in the pools of DOC and PCHO was observed with the onset of nutrient limitation. Moreover, raising the temperature by up to 8°C also notably accelerated the rate at which polysaccharides accumulated by a factor of 4 under these nutrient conditions. In contrast, the rise in dissolved C compound concentration was considerably less pronounced in the low-N microcosms and did not respond significantly to warming. Together, these findings strongly suggest a distinct, temperature-driven shift in the partitioning of organic C between particulate and dissolved pools under N-replete conditions. The timing of the accumulation as well as the increasing proportion of polysaccharides, which have been shown to comprise a major fraction of freshly produced algal exudates (Benner et al. 1992; Biddanda and Benner 1997; Biersmith and Benner 1998), suggests that exudation by phytoplankton cells due to a cellular overflow of excess photosynthates was one of the primary sources, and similar observations have been made frequently in laboratory and mesocosm studies (Myklestad 1995; Norrman et al. 1995; Obernosterer and Herndl 1995).

This mechanism, however, cannot alone account for the observed pronounced temperature-dependence of PCHO accumulation because both autotrophic primary production and biomass accumulation did not respond notably to experimental warming during our study. Alternatively, also a temporal decoupling of autotrophic production and heterotrophic consumption processes, which has been attributed to a partly low degradability of the accumulating matter (Fry et al. 1996) or an inefficient bacterial utilization of these compounds due to nutrient limitation (Thingstad et al. 1997), may have contributed to the increase in DOC and PCHO observed herein. This is, in fact, supported by the pronounced decline in the activity ratio of the bacterial extracellular enzymes leu-amp and BOC-pep, indicating a shift in the relative use of short-chained over more complex, long-chained peptides, as well as the enhanced activity of the DOP-cleaving enzyme APA in response to warming. However, similar to the temperature-insensitivity of algal primary production, these mechanisms would only have resulted in an accumulation of the released material, with the initiation of DOC accumulation being dependent on the onset of nutrient limitation.

This clearly points to the presence of another, temperature-sensitive process contributing to the enhanced accumulation of DOC and PCHO at elevated temperature. Several studies have reported that bacteria may themselves produce copious amounts of slowly degradable DOC (Brophy and Carlson 1989; Ogawa et al. 2001; Kawasaki and Benner 2006). The potential mechanisms of bacterial DOC release include the partial hydrolysis of polymeric substances (Azam 1998), as well as the release of a polysaccharide-rich matrix, which is often surrounding bacterial cells (Heissenberger et al. 1996) and has been shown to be constantly renewed during growth (Stoder-

egger and Herndl 1998). Metabolically active bacteria may, thus, rather contribute to the accumulation of DOC than to its consumption. These findings suggest that the observed stimulation of bacterial activities by rising temperature likely contributed significantly to the temperature-dependent increase in DOC and PCHO concentrations under N-replete conditions in our study. In addition, also viral cell lysis, although not investigated in this study, may have influenced the observed DOC dynamics.

Interactive effects of rising sea-surface temperature and nutrient stoichiometry, and their potential implications for future elemental cycling—In the present study, the combined effects of increasing temperature and either N-replete or -deficient growth conditions exerted a strong effect on the cycling of organic matter in an algal–bacterial assemblage due to strongly diverging temperature-response patterns of the investigated community under the two respective nutrient situations. While the net build-up of autotrophic biomass remained largely unaffected by temperature in both N : P treatments, the bacterial communities displayed marked changes in their activity patterns, with a pronounced stimulation of bacterial biomass production and hydrolytic enzyme activities by increasing temperature under high-N conditions compared to a weak (e.g., BSP) or even absent (e.g., extracellular enzyme activities) temperature response in the low-N microcosms.

Considering these nutrient-related differences in the reaction of an algal–bacterial community to experimental warming, it may be illustrative to consider the cellular functions and utilization of P and N compounds in more detail. While cell-bound N is mainly present in the form of proteins, the most P-rich cellular compound is ribonucleic acid (RNA), constituting a major fraction of ribosomes, the cellular organelles responsible for protein synthesis and, thus, for growth (Geider and LaRoche 2002). Ribosomes also contain, however, approximately one-third protein by weight (Geider and LaRoche 2002). From a simplistic point of view, the cellular allocation of nutrients can be divided into an assembly machinery (i.e., ribosomes), and a resource acquisition machinery (e.g., proteins for nutrient uptake enzymes or photosynthetic pigments). While the first is rich in P, but also contains N in notable amounts, the latter is rich in N with little or no P. The N-replete conditions investigated in this study, thus, may have limited microorganism growth in producing sufficient amounts of RNA for the synthesis of new ribosomes. On the other hand, the stimulation of bacterial activities by experimental warming likely led to an increased remineralization of P compounds, thereby refueling the algal–bacterial community with pulses of bioavailable P and alleviating the P deficiency. In contrast, organisms experiencing N-deficient conditions may have been constrained in their activity and growth in two ways, because they may either have channeled the sparse N into the synthesis of ribosomes, being a prerequisite for the assembly of proteins and enzymes necessary for various cellular functions, or into the resource acquisition machinery, which is, for instance, responsible for energy supply via light-harvesting pigments. Thus, the allocation of N to one compartment may ultimately restrict the resource availability for the other compartment within an organism, thereby hindering important cellular functions and reducing the overall activity and response potential to other environmental factors, as for instance temperature. In support of this, the lower POC-normalized build-up of Chl *a* in the low- compared to the high-N treatments indeed suggests that the former community allocated comparatively fewer resources per biomass into the production of pigments and the acquisition of energy.

The differential behavior of the bacterial community to increasing temperature further translated into distinct shifts in the build-up and partitioning of organic matter. Under N-deficient growth conditions, organic C accumulating in the water column was mostly present in particulate form and the concentration of DOC remained fairly low. If applied to the surface ocean, this may, together with the observed restricted microbial degradation, facilitate the efficient utilization of the produced organic matter in the pelagic food web and its sedimentation to depth. Contrastingly, rising temperature clearly shifted the overall partitioning of organic C between the particulate and dissolved pools toward an increasing accumulation of dissolved C-rich compounds and led to an accelerated degradation of POC, as well as likely also to a rapid remineralization and reutilization of P under the respective N-replete conditions.

In concert, the changes observed herein in organic matter cycling with a shift from N-deficient to -replete conditions strongly indicate an increased flow of energy and matter through the microbial loop, hence diverting the accumulating organic matter away from transfer to higher trophic levels and also from export to deeper water layers. This may not only profoundly affect the structure of pelagic food webs, but also has the potential to reduce the transport of biogenic matter to depth via the biological C pump—with likely consequences for the ocean's mitigating role in Earth's climate system.

Acknowledgments

We thank A. Ludwig and P. Fritsche for technical assistance. This work is a contribution to the priority program 1162 'AQUASHIFT' and the Sonderforschungsbereich 754 'Climate-Biogeochemistry interactions in the tropical ocean' funded by the Deutsche Forschungsgemeinschaft (DFG). The constructive comments of two anonymous reviewers are gratefully acknowledged.

References

Ammerman, J. W., R. R. Hood, D. A. Case, and J. B. Cotner. 2003. Phosphorus deficiency in the Atlantic: An emerging paradigm on oceanography. EOS **84:** 170, doi:10.1029/2003EO180001

Azam, F. 1998. Microbial control of oceanic carbon flux: The plot thickens. Science **280:** 694–696, doi:10.1126/science.280.5364.694

Barcelos e Ramos, J., H. Biswas, K. G. Schulz, J. LaRoche, and U. Riebesell. 2007. Effect of rising atmospheric carbon dioxide on the marine nitrogen fixer *Trichodesmium*. Glob. Biogeochem. Cycles **21:** GB2028, doi:10.1029/2006GB002898

Barnett, T. P., D. W. Pierce, K. M. Achutarao, P. J. Gleckler, B. D. Santer, J. M. Gregory, and W. M. Washington. 2005. Penetration of human-induced warming into the world's oceans. Science **309:** 284–287, doi:10.1126/science.1112418

Benner, R., J. D. Pakulski, M. Mccarthy, J. I. Hedges, and P. G. Hatcher. 1992. Bulk chemical characteristics of dissolved organic matter in the ocean. Science **255:** 1561–1564, doi:10.1126/science.255.5051.1561

Biddanda, B., and R. Benner. 1997. Carbon, nitrogen and carbohydrate fluxes during the production of particulate and dissolved organic matter by marine phytoplankton. Limnol. Oceanogr. **42:** 506–518, doi:10.4319/lo.1997.42.3.0506

Biersmith, A., and R. Benner. 1998. Carbohydrates in phytoplankton and freshly produced dissolved organic matter. Mar. Chem. **63:** 131–144, doi:10.1016/S0304-4203(98)00057-7

Boyd, P. W., and S. C. Doney. 2002. Modelling regional responses by marine pelagic ecosystems to global climate change. Geophys. Res. Lett. **29:** 1806, doi:10.1029/2001GL014130

Breithaupt, P. 2009. The impact of climate change on phytoplankton–bacterioplankton interactions. Ph.D. thesis. Christian-Albrechts-Universität, Kiel, Germany.

Brophy, J. E., and D. J. Carlson. 1989. Production of biologically refractory dissolved organic carbon by natural seawater microbial populations. Deep-Sea Res. Part 1: Oceanogr. Res. Pap. **36:** 497–507, doi:10.1016/0198-0149(89)90002-2

Caldeira, K., and M. E. Wickett. 2003. Anthropogenic carbon and ocean pH. Nature **425:** 365, doi:10.1038/425365a

Edwards, M., and A. J. Richardson. 2004. Impact of climate change on marine pelagic phenology and trophic mismatch. Nature **430:** 881–884, doi:10.1038/nature02808

Falkowski, P. G. 1997. Evolution of the nitrogen cycle and its influence on the biological sequestration of CO_2 in the ocean. Science **387:** 272–275.

———, and others. 2000. The global carbon cycle: A test of our knowledge of earth as a system. Science **290:** 291–296, doi:10.1126/science.290.5490.291

Feely, R. A., S. C. Doney, and S. R. Cooley. 2009. Ocean acidification—present conditions and future changes in a high-CO_2 world. Oceanography **22:** 36–47.

Fry, B., C. S. J. Hopkinson, A. Nolin, B. Norrmann, and U. L. Zweifel. 1996. Long-term decomposition of DOC from experimental diatom blooms. Limnol. Oceanogr. **41:** 1344–1347, doi:10.4319/lo.1996.41.6.1344

Geider, R. J., and J. LaRoche. 2002. Redfield revisited: Variability of C : N : P in marine microalgae and its biochemical basis. Eur. J. Phycol. **37:** 1–17, doi:10.1017/S0967026201003456

Giorgi, F., and others. 2001. Regional climate information—evaluation and projections, p. 881. *In* J. T. Houghton, Y. Ding, D. J. Griggs, M. Noguer, P. J. van der Linden, X. Dai, K. Maskell, and C. A. Johnson [eds.], Climate change 2001: The scientific basis. Contribution of Working Group I to the Third Assessment Report of the Intergovernmental Panel on Climate Change. Cambridge Univ. Press.

Guillard, R. L. R., and J. H. Ryther. 1962. Studies of marine planktonic diatoms. I. *Cyclotella nana* (Hustedt) and *Detonula confervacea* (Cleve). Can. J. Microbiol. **8:** 229–239, doi:10.1139/m62-029

Hansen, H. P., and F. Koroleff. 1999. Determination of nutrients, p. 159–228. *In* K. Grasshoff, K. Kremling, and M. Ehrhardt [eds.], Methods of seawater analysis. Wiley VCH.

Heissenberger, A., G. G. Leppard, and G. J. Herndl. 1996. Relationship between the intracellular integrity and the morphology of the capsular envelope in attached and free-living marine bacteria. Appl. Environ. Microbiol. **62:** 4521–4528.

Holmes, R. M., A. Aminot, R. Kéroule, B. A. Hooker, and B. J. Peterson. 1999. A simple and precise method for measuring ammonium in marine and freshwater ecosystems. Can. J. Fish. Aquat. Sci. **56:** 1801–1808, doi:10.1139/cjfas-56-10-1801

Hoppe, H. G. 1983. Significance of exoenzymatic activities in the ecology of brackish water: Measurements by means of methylumbelliferyl-substrates. Mar. Ecol. Prog. Ser. **11:** 299–308, doi:10.3354/meps011299

Hutchins, D. A., and others. 2007. CO_2 control of *Trichodesmium* N_2 fixation, photosynthesis, growth rates, and elemental ratios: Implications for past, present, and future ocean biogeochemistry. Limnol. Oceanogr. **52:** 1293–1304.

Jickells, T. D. 1998. Nutrient biogeochemistry of the coastal zone. Science **281:** 217–222, doi:10.1126/science.281.5374.217

Karl, D. M., and others. 2001. Ecological nitrogen-to-phosphorus stoichiometry at station ALOHA. Deep-Sea Res. Part II **48:** 1529–1566, doi:10.1016/S0967-0645(00)00152-1

Kawasaki, N., and R. Benner. 2006. Bacterial release of dissolved organic matter during cell growth and decline: Molecular origin and composition. Limnol. Oceanogr. **51:** 2170–2180, doi:10.4319/lo.2006.51.5.2170

Levitus, S., J. Antonov, and T. Boyer. 2005. Warming of the world ocean 1955–2003. Geophys. Res. Lett. **32:** L02604, doi:10.1029/2004GL021592

Magaletti, E., R. Urbani, P. Sist, C. R. Ferrari, and A. M. Cicero. 2004. Abundance and chemical characterization of extracellular carbohydrates released by the marine diatom *Cylindrotheca fusiformis* under N- and P-limitation. Eur. J. Phycol. **39:** 133–142, doi:10.1080/0967026042000202118

Meehl, G. A., and others. 2007. Global climate projections, p. 747–845. *In* S. Solomon, M. M. D. Qin, Z. Chen, M. Marquis, K. B. Averyt, M. Tignor, and H. L. Miller [eds.], Climate change 2007: The physical science basis. Contribution of Working Group I to the Fourth Assessment Report of the Intergovernmental Panel on Climate Change. Cambridge Univ. Press.

Myklestad, S. 1995. Release of extracellular products by phytoplankton with special emphasis on polysaccharides. Sci. Total Environ. **165:** 155–164, doi:10.1016/0048-9697(95)04549-G

———, E. Skånøy, and S. Hestmann. 1997. A sensitive and rapid method for analysis of dissolved mono- and polysaccharides in seawater. Mar. Chem. **56:** 279–286, doi:10.1016/S0304-4203(96)00074-6

Norrman, B., U. L. Zweifel, C. S. Hopkinson, and B. Fry. 1995. Production and utilization of dissolved organic carbon during an experimental diatom bloom. Limnol. Oceanogr. **40:** 898–907, doi:10.4319/lo.1995.40.5.0898

Obernosterer, I., and G. J. Herndl. 1995. Phytoplankton extracellular release and bacterial growth: Dependence on the inorganic N : P ratio. Mar. Ecol. Prog. Ser. **116:** 247–257, doi:10.3354/meps116247

Ogawa, H., Y. Amagai, I. Koike, K. Kaiser, and R. Benner. 2001. Production of refractory dissolved organic matter by bacteria. Science **292:** 917–920, doi:10.1126/science.1057627

Puddu, A., A. Zoppini, S. Fazi, M. Rosati, S. Amalfitano, and E. Magaletti. 2003. Bacterial uptake of DOM released from P-limited phytoplankton. FEMS Microbiol. Ecol. **46:** 257–268.

Qian, J., and K. Mopper. 1996. Automated high-performance, high-temperature combustion total organic carbon analyzer. Anal. Chem. **68:** 3090–3097, doi:10.1021/ac960370z

Redfield, A. C., B. M. Ketchum, and F. A. Richards. 1963. The influence of organism on the composition of sea-water, p. 26–77. *In* M. N. Hill [ed.], The sea. Wiley.

Sarmiento, J. L., T. M. C. Hughes, R. J. Stouffer, and S. Manabe. 1998. Simulated response of the ocean carbon cycle to anthropogenic climate warming. Nature **393:** 245–249, doi:10.1038/30455

Sharp, J. H. 1974. Improved analysis for particulate organic carbon and nitrogen from seawater. Limnol. Oceanogr. **19:** 984–989, doi:10.4319/lo.1974.19.6.0984

Simon, M., and F. Azam. 1989. Protein content and protein synthesis rates of planktonic marine bacteria. Mar. Ecol. Prog. Ser. **51:** 201–213, doi:10.3354/meps051201

Sommer, U., and K. Lengfellner. 2008. Climate change and the timing, magnitude, and composition of the phytoplankton spring bloom. Glob. Change Biol. **14:** 1199–1208, doi:10.1111/j.1365-2486.2008.01571.x

Stoderegger, K., and G. J. Herndl. 1998. Production and release of bacterial capsular material and its subsequent utilization by marine bacterioplankton. Limnol. Oceanogr. **43:** 877–884, doi:10.4319/lo.1998.43.5.0877

Thingstad, T. F., A. Hagstrom, and F. Rassoulzadegan. 1997. Accumulation of degradable DOC in surface waters: Is it caused by a malfunctioning microbial loop? Limnol. Oceanogr. **42:** 398–404, doi:10.4319/lo.1997.42.2.0398

———, and others. 2005. Nature of phosphorus limitation in the ultraoligotrophic Eastern Mediterranean. Science **309:** 1068–1071, doi:10.1126/science.1112632

Trenberth, K. E., and others. 2007. Observations: Surface and atmospheric climate change, p. 235–336. *In* S. Solomon, M. M. D. Qin, Z. Chen, M. Marquis, K. B. Averyt, M. Tignor, and H. L. Miller [eds.], Climate change: The physical science basis. Contribution of Working Group I to the Fourth Assessment Report of the Intergovernmental Panel on Climate Change. Cambridge Univ. Press.

Tyrrell, T. 1999. The relative influences of nitrogen and phosphorus on oceanic primary production. Nature **400:** 525–531, doi:10.1038/22941

Utermöhl, H. 1958. Zur Vervollkommnung der quantitativen Phytoplankton-Methodik. Mitt. Int. Ver. Theor. Angew. Limnol. **9:** 263–272.

Welschmeyer, N. A. 1994. Fluorometric analysis of chlorophyll *a* in the presence of chlorophyll *b* and pheopigments. Limnol. Oceanogr. **39:** 1985–1992, doi:10.4319/lo.1994.39.8.1985

Wohlers, J., and others. 2009. Changes in biogenic carbon flow in response to sea surface warming. Proc. Natl. Acad. Sci. USA **106:** 7067–7072, doi:10.1073/pnas.0812743106

Zweifel, U. L., B. Norrman, and Å. Hagström. 1993. Consumption of dissolved organic carbon by marine bacteria and demand for inorganic nutrients. Mar. Ecol. Prog. Ser. **101:** 23–32, doi:10.3354/meps101023

Associate editor: Michael R. Landry

Received: 13 April 2010
Accepted: 02 November 2010
Amended: 13 December 2010